Environmental Modelling & Software 24 (2009) 530–541

Contents lists available at ScienceDirect

Environmental Modelling & Software

journal homepage: www.elsevier.com/locate/envsoft

Stochastic sampling design using a multi-objective genetic algorithm and adaptive neural networks

Kourosh Behzadian [a], Zoran Kapelan [b,*], Dragan Savic [b], Abdollah Ardeshir [c]

[a] Environmental Research Center, Amirkabir University of Technology, 424, Hafez Ave.– P.O. Box 15875-4413 Tehran, Iran
[b] Centre for Water Systems, University of Exeter, Harrison Building, North Park Road, EX4 4QF Exeter, United Kingdom
[c] Department of Civil and Environmental Engineering, Amirkabir University of Technology, 424, Hafez Ave. P.O. Box 15875-4413 Tehran, Iran

ARTICLE INFO

Article history:
Received 1 April 2008
Received in revised form
29 September 2008
Accepted 30 September 2008
Available online 22 November 2008

Keywords:
Water distribution system
Calibration
Uncertainty
Multi-objective genetic algorithm
Adaptive neural networks

ABSTRACT

This paper presents a novel multi-objective genetic algorithm (MOGA) based on the NSGA-II algorithm, which uses metamodels to determine optimal sampling locations for installing pressure loggers in a water distribution system (WDS) when parameter uncertainty is considered. The new algorithm combines the multi-objective genetic algorithm with adaptive neural networks (MOGA–ANN) to locate pressure loggers. The purpose of pressure logger installation is to collect data for hydraulic model calibration. Sampling design is formulated as a two-objective optimization problem in this study. The objectives are to maximize the calibrated model accuracy and to minimize the number of sampling devices as a surrogate of sampling design cost. Calibrated model accuracy is defined as the average of normalized traces of model prediction covariance matrices, each of which is constructed from a randomly generated sampling set of calibration parameter values. This method of calculating model accuracy is called the 'full' fitness model. Within the genetic algorithm search process, the full fitness model is progressively replaced with the periodically (re)trained adaptive neural network metamodel where (re)training is done using the data collected by calling the full model. The methodology was first tested on a hypothetical (benchmark) problem to configure the setting requirement. Then the model was applied to a real case study. The results show that significant computational savings can be achieved by using the MOGA–ANN when compared to the approach where MOGA is linked to the full fitness model. When applied to the real case study, optimal solutions identified by MOGA–ANN are obtained 25 times faster than those identified by the full model without significant decrease in the accuracy of the final solution.

1. Introduction

Data for the calibration of a water distribution system (WDS) model is usually collected from a series of field tests at strategic locations within the network in which the pressure head is recorded (de Schaetzen et al., 2000). The accuracy of calibration depends on the quality and quantity of the collected data and its relative location to the calibration parameters being estimated. Therefore, the selection of appropriate collection locations, called the sampling design (SD), is important and has been a challenge for researchers and practitioners (Kapelan et al., 2005a).

Practitioners often use a simplified approach for sampling design since they seek straightforward applicable methods without the need for complex computations (Walski, 1983). Although these methods are simple to understand and apply, they suffer from the lack of accuracy since they may require a logger to be located on nodes where pressures are insensitive with respect to calibration parameters. This way, the measurement locations that can return most of the information about calibration parameters may be easily omitted.

The above problem was overcome in the past by identifying sampling designs that have the optimal trade-off between calibrated model accuracy and the sampling design cost (Meier and Barkdoll, 2000; de Schaetzen et al., 2000; Kapelan et al., 2003; Vitkovsky et al., 2003). However, all these models require estimating the calibration parameter values prior to the optimization-based sampling design process. This is difficult to achieve as these values can be obtained accurately only after the model calibration.

To overcome this problem, a stochastic sampling design problem is formulated and solved here. The problem is formulated as an optimization problem trading off the calibrated model accuracy with the sampling design cost but this time, calibration parameter values are assumed uncertain and modelled by using probability density functions. This way, a more realistic

* Corresponding author. Tel.: +44 1392 264054; fax: +44 1392 217965.
E-mail address: z.kapelan@exeter.ac.uk (Z. Kapelan).

1364-8152/$ – see front matter © 2008 Elsevier Ltd. All rights reserved.
doi:10.1016/j.envsoft.2008.09.013

Nomenclature

a	vector of calibration parameters
Δa	perturbation value added to a_k
$\mathbf{Cov}_a$	parameter variance–covariance matrix
$\mathbf{Cov}_z$	model prediction variance–covariance matrix
F_1	normalized first objective function
F_2	normalized second objective function
f_1	average of model prediction uncertainty
s	standard deviation of measurement devices
$f_{1,ml}$	value of f_1 assuming that all analysed locations are monitored
ITG	Initial Training Generations
$\mathbf{J}$	Jacobian matrix
$\mathbf{J}_{ml}$	full Jacobian matrix (all locations monitored)
$\mathbf{J}_z$	prediction Jacobian matrix
NF	number of best Pareto (sub)fronts in offspring population
N_a	number of calibration parameters
N_k	number of sets of samples from uncertain parameters
N_l	actual number of measurement devices
$N_l^{\max}$	maximum allowed number of measurement devices
$N_l^{\min}$	minimum number of measurement devices
N_{ml}	number of SD potential measurement locations
N_o	number of measurements in both spatial and temporal domain
N_z	number of model predictions for whom uncertainty are evaluated

Superscript

T	vector/matrix transpose operator
s	standard deviation of measurement devices
y	vector of WDS model predicted variables
z	vector of model predictions of interest

representation of the (essentially unknown) calibration parameter values is obtained which should lead to more robust sampling designs obtained. However, this comes at the price as stochastic sampling design problem is more difficult to solve than the deterministic one.

In this paper, an overview of sampling design and metamodelling approaches is briefly presented first. Optimal sampling design problem is then formulated. Following this, the methodology of the proposed algorithm, i.e. the multi-objective genetic algorithm and the adaptive neural network (MOGA–ANN), is described. The MOGA–ANN for SD is first tested on a hypothetical WDS, which is often used as a benchmark problem (Farmani et al., 2003), and then it is applied to a real case study. Finally, the relevant conclusions are drawn.

2. Background

2.1. Sampling design

The problem of sampling design for WDS model calibration has attracted the attention of a number of researchers in recent years (Kapelan, 2002; Lansey, 2006). Only a few recently developed studies related to the proposed model are discussed here. A comprehensive overview of the relevant works can be found in Kapelan (2002).

Most of the developed SD approaches have been based on the sensitivity criteria of measurement locations with respect to calibration parameters. Mainly, Jacobian matrix and covariance matrix are used to find the most sensitive locations for monitoring (Yu and Powell, 1994; Bush and Uber, 1998; Lansey et al., 2001; Kapelan et al., 2003). These criteria have been used either to rank potential locations based on a sensitivity-based method (Ferreri et al., 1994; Bush and Uber, 1998; Piller et al., 1999) or to create an optimization problem (Lee and Deininger, 1992; Meier and Barkdoll, 2000; de Schaetzen et al., 2000; Kapelan et al., 2003; Vitkovsky et al., 2003).

In the above ranking type approaches, a new measurement location leading to the current largest increase in SD accuracy is added to the previously selected set of logger locations until the maximum number of loggers is reached. This implies that the optimal set for N measurement locations is always a superset of the optimal set for $N-1$ locations, which was shown not to be always true (Kapelan et al., 2003). Having said this, when compared to the empirical methods, the ranking type approach is computationally superior and easy to set up as it does not require solving a complex optimization problem.

The optimization model can take into account the effect of a set of monitoring locations altogether and their mutual interactions when performing SD for a set of specified monitoring locations. Most SD approaches have used genetic algorithms (GAs) to solve the associated optimization problem (Meier and Barkdoll, 2000; de Schaetzen et al., 2000; Kapelan et al., 2003; Vitkovsky et al., 2003).

Bush and Uber (1998) proposed three sensitivity-based methods to rank the locations of pressure and tracer measurements within WDS for model calibration. All three methods are based on minimizing the uncertainty in estimated parameter values (directly or indirectly). Lansey et al. (2001) developed an SD procedure based on a three-step calibration process to consider the uncertainties in measurement and estimation. The trace of the model prediction covariance matrix is used as the model uncertainty. They finally proposed how to identify the preferable conditions and locations for data collection based on the uncertainty and sensitivity-based heuristic analysis.

The model by Kapelan et al. (2003) presented a deterministic multi-objective genetic algorithm (MOGA) for SD prior to WDS model calibration. The two objectives proposed were to maximize calibrated model accuracy and to minimize total SD costs. The authors also proposed and compared three different approaches for evaluating the model accuracy, which were calculated using some norms of the parameter itself or the prediction covariance matrix. In this approach, elements of the Jacobian matrix are calculated prior to the optimization model run by assuming the model parameter values. This approach is obviously prone to errors as that kind of information is not readily available when measurement locations are being selected.

In water quality management, optimal sensor placement in WDS has also attracted special attention with the aim of identifying contamination sources (Ostfeld and Salomons, 2004; Berry et al., 2005, 2006; Propato, 2006; Shastri1 and Diwekar, 2006). They all typically minimize the risk from contamination using sensors for timely detection.

2.2. Metamodelling

The use of metamodels to reduce the computational times in optimization processes was proposed by Blanning (1975). A metamodel can be used as a surrogate for calculating fitness values, which are normally based on time-consuming simulations. Such a metamodel can be effectively integrated into the search process to gradually substitute the large portion of simulation which model runs require. One of the frequently used metamodels is the artificial

neural network (ANN) because of its ability to approximate effectively a wide range of non-linear functions (Leshno et al., 1993).

Historically, ANNs have been successfully applied to several water resource problems, such as groundwater remediation designs (Aly and Peralta, 1999; Yan and Minsker, 2006), water distribution systems (Lingireddy and Ormsbee, 1998; Broad et al., 2005; May et al., 2008), river sediment load estimation (Alp and Cigizoglu, 2007) and coastal pollution prediction (Lin et al., 2008). In a recent application of groundwater remediation design, Yan and Minsker (2006) reported a model that makes use of an adaptive neural network and a single objective genetic algorithm. They saved approximately 90 percent of the simulation model calls with no loss in accuracy in the optimal solutions. In the context of water distribution systems Lingireddy and Ormsbee (1998) applied ANNs to optimal calibration of a WDS model. Later, Broad et al. (2005) proposed ANNs as a substitution for a complex simulation model for WDS design, in which ANNs were trained offline. As ANNs were trained before being used by the optimization model, the authors proposed setting some heuristic rules to prohibit solutions becoming infeasible. In a recent application, May et al. (2008) developed ANN models to forecast water quality within water distribution systems. They proposed a new non-linear input variable selection algorithm to reduce arbitrary judgement and extensive trial-and-error during ANN training.

3. Optimal sampling design

The objective of the SD here is to find a set of optimal measurement locations with the aim of calibrating accurately the WDS hydraulic model. These models are typically calibrated for uncertain pipe roughness coefficients and nodal demands, often jointly for both (Walski, 1983, 1986; Bhave, 1988; Ormsbee, 1989; Lansey and Basnet, 1991). Other sources of uncertainty (i.e. potential calibration parameters) may exist too, e.g. nodal elevation errors, tank level errors, level of detail (skeletonisation) errors, outdated pump curves, to name the few (AWWA, 1999). Pipe roughness coefficient values are usually estimated because it is usually too difficult/costly to inspect the condition of underground pipes. On the other hand, demands are calibrated because they are often not monitored (at least not in the UK). Even when they are monitored, an error is introduced when actual demands of individual households (that occur along the pipe/street) are lumped together to a nearby network node to construct a WDS model.

The stochastic SD problem is formulated and solved here as a two-objective optimization problem under parameter uncertainty. The two objectives are the maximization of the calibrated model accuracy and the minimization of the sampling design cost.

To quantify the calibrated model prediction accuracy, a first-order second-moment (FOSM) model is used to approximate the relevant parameter and prediction covariance matrices. Without the loss of generality, it is assumed that prediction and measurement variables of interest are nodal pressures only. As a consequence, if a set of N_l measurement devices with the standard deviation of s are installed in N_l measurement WDS locations, the variance of calibrated parameters can be estimated from the diagonal elements of the parameter covariance matrix (Bush and Uber, 1998; Kapelan et al., 2005a):

$$\mathbf{Cov}_a = s^2\left(\mathbf{J}^{\mathrm{T}}\mathbf{J}\right)^{-1} \tag{1}$$

where $\mathbf{J}$ = Jacobian matrix of derivatives $\partial y_i/\partial a_k$ ($i = 1,\ldots,N_o$; $k = 1,\ldots,N_a$), y = vector of N_o pressure predictions at locations where loggers are installed, a = vector of N_a calibration parameters, N_o = number of observations, i.e. measurement data in both spatial and temporal domains (e.g. if there are N_t time steps for each of N_l monitoring locations, then $N_o = N_t \cdot N_l$), N_a = number of calibration parameters. Note that the above equation can be used to propagate uncertainty in any measurements (e.g. pressures and/or flows) to any calibration parameters (e.g. pipe roughness coefficients and nodal demands). It captures the relative sensitivity of estimated calibration parameters to the measurements used. This sensitivity depends on a number of factors including relative proximity of measurement locations to estimated calibration parameters, calibration parameter grouping (if any), flow conditions in the network during field tests, etc. As a consequence, it is very difficult to state upfront which parameters (e.g. pipe roughnesses or nodal demands) will be more sensitive to the measurements collected (e.g. pressures).

Once the parameter uncertainties are estimated using equation (1), the uncertainty in calibrated model predictions (e.g. pressures) at any location in the system can be estimated from the diagonal elements of the prediction covariance matrix (Lansey et al., 2001; Kapelan et al., 2005a):

$$\mathbf{Cov}_z = \mathbf{J}_z \cdot \mathbf{Cov}_a \cdot \mathbf{J}_z^{\mathrm{T}} \tag{2}$$

where $\mathbf{J}_z$ = Jacobian matrix of derivatives $\partial z_i/\partial a_k$ ($i = 1,\ldots,N_z$; $k = 1,\ldots,N_a$); z = vector of N_z pressure predictions of interest. Note that there are several general methods for the calculation of Jacobian matrices $\mathbf{J}$ and $\mathbf{J}_z$ (Kapelan et al., 2003). Here, the elements of these two matrices are calculated by using the finite difference method (Lansey et al., 2001):

$$\frac{\partial z_i}{\partial a_k} = \frac{z_i^{\Delta} - z_i}{(a_k + \Delta a) - a_k} \tag{3}$$

where z_i^{Δ} = pressure prediction with the perturbed calibration parameter value $(a_k + \Delta a)$; z_i = pressure prediction with the assumed calibration parameter value a_k; and Δa = perturbation value added to a_k. To calculate the elements of the Jacobian matrix, the following procedure needs to be used: (1) simulate the hydraulic model by using the assumed parameter value; (2) simulate the hydraulic model by using the perturbed calibration parameter value, $a_k + \Delta a$, for $k = 1$; (3) calculate derivatives by using equation (3) and complete the first row of the Jacobian matrix; and (4) repeat steps 2 and 3 for $k = 2, \ldots, N_a$.

To aggregate the model prediction uncertainty, the average of square root of all diagonal elements in matrix $\mathbf{Cov}_z$ (i.e. standard deviations of model predictions) is assumed as the model uncertainty:

$$f_1 = \frac{1}{N_z}\sum_{i=1}^{N_z} \mathbf{Cov}_{z,ii}^{1/2} \tag{4}$$

Therefore, the normalized prediction accuracy is then defined as follows (Kapelan et al., 2003; Bush and Uber, 1998):

$$F_1 = \frac{f_{1,ml}}{f_1} \tag{5}$$

where $f_{1,ml}$ = the value of model uncertainty for the ideal state where all potential measurement locations are monitored. Note that if model uncertainty (equation (4)) is to be minimized then normalized prediction accuracy (equation (5)) has to be maximized.

Note that all N_a calibration parameters have to be assigned a value before the values of the full Jacobian matrix can be calculated, i.e. before sampling design process can commence. These values, however, are not normally available prior to the sampling design process. To overcome this problem, each calibration parameter is assumed here to be uncertain following some predefined probability density function (PDF). It is envisaged that this

should enable a more realistic representation of essentially unknown calibration parameter values.

As a consequence, the calibration accuracy objective is defined here as the average of normalized prediction accuracies (see equation (5)), each of which is constructed from a randomly generated sample of calibration parameter values:

$$\text{Maximize } F_1 = \frac{1}{N_k}\sum_{j=1}^{N_k}\frac{f_{1,ml}^{j}}{f_1^{j}} \tag{6}$$

where N_k = number of sets of samples and superscript j refers to jth sampling set. This approach to calculating the first objective value is called the 'full' fitness model henceforth. To do so, N_k sets of uncertain parameter values are randomly generated from the associated PDFs by using the Latin Hypercube (LH) sampling technique (McKay et al., 1979; Helton and Davis, 2003; Post et al., 2008). The noisy objective value is then calculated by averaging the relative accuracies obtained by N_k runs of the deterministic SD model.

The sampling design cost is surrogated by the number of devices used leading to the following second optimization objective and the associated constraint:

$$\text{Minimize } F_2 = N_l/N_{ml} \tag{7}$$

$$N_l^{\min} \le N_l \le N_l^{\max} \tag{8}$$

where N_{ml} = number of potential measurement locations; $N_l^{\min}$, $N_l^{\max}$ = minimum and maximum number of measurement devices used, respectively.

4. Methodology

The objectives and the constraints shown in equations (6)–(8) define a two-objective optimization problem under uncertainty. The main problem here is how to efficiently calculate the value of first objective function (see equation (6)) due to the time consuming nature of repetitive Jacobian matrix calculations. To resolve this, the optimization problem is solved by using the multi-objective genetic algorithm coupled with adaptive neural networks (MOGA–ANN).

Each GA chromosome is coded as a potential sampling design solution and its fitness is evaluated initially by using the full fitness model (i.e. with a number of samples). Later on, during the GA search process, the full fitness model is progressively replaced with the periodically (re)trained ANN metamodel where (re)training is done using the data collected from the previous evaluations by the full model. The ANN is retrained after a pre-specified number of objective function evaluations using the full model. The detailed flowchart of MOGA–ANN is shown in Fig. 1.

4.1. Multi-objective genetic algorithm

Here, a multi-objective evolutionary algorithm known as the Non-dominated Sorting Genetic Algorithm II (NSGA-II) is used (Deb et al., 2002). NSGA-II alleviates all of the following difficulties of previous MOGAs: (1) considerable computational effort, (2) non-elitism approach, and (3) the need for the specification of a sharing parameter. The selection operator in NSGA-II combines the parent and offspring populations in a single population and then selects the best solutions with respect to fitness and spread criteria. More details of this approach can be found in Deb et al. (2002).

Integer value coding is used for the encoding of each chromosome. The number of genes equals the maximum number of measurement devices ($N_l^{\max}$), each of which represents the position of one pressure logger in WDS. A gene with zero value indicates no measurement device is available. When using integer encoding, two or more genes may take the same integer value, indicating more than one pressure logger should be installed in the same location. These solutions will be rejected by MOGA due to an increase in cost and no increase in accuracy (Kapelan, 2002).

4.2. Artificial neural network (ANN)

The ANN is used here as a replacement for a full fitness evaluation model used when estimating the model accuracy objective with the idea of making significant computational time savings. However, ANN predictions are only approximate and, therefore, prone to errors when used to evaluate the objective value. To resolve this problem, several strategies have been proposed to sample solutions and calculate the relevant objective value with the full model. In addition, the ANNs are periodically retrained within the algorithm progress to improve their prediction accuracy.

Fig. 2 shows the architecture of the proposed ANN. As it can be seen, a conventional neural network with an input, hidden and an output layer is assumed. Input data are defined as measurement locations, hence the number of input layer neurons is equal to the maximum number of measurement devices (see above). The output layer has one neuron only equal to the value of first objective function (prediction accuracy), as defined in equation (6). The second objective function value, i.e. the number of measurement locations, is directly calculated and there is no need to consider it as an additional output neuron. The back propagation Levenberg–Marquardt algorithm is used to train the ANN (Lingireddy and Ormsbee, 1998).

4.3. MOGA–ANN algorithm

A flowchart of the proposed MOGA–ANN method is shown in Fig. 1. It can be seen that the method is essentially a modified NSGA-II algorithm that makes use of the ANN and the caching technique. The search process starts by creating a random initial population and evaluating the fitness of each chromosome by using the full fitness evaluation model. The data obtained (both chromosome components, i.e. genes and relevant objective function values) is then stored in the cache with the idea of preventing costly repetitive fitness evaluations. The cache is updated continuously during the search process, i.e. every time chromosome fitness is evaluated using the full model.

The main loop of the algorithm starts with the creation of the offspring population using the NSGA-II selection, crossover, and mutation operators. In the first few generations, chromosome fitness is estimated using the full model only, in order to collect enough ANN training data (steps 5–7 in Fig. 1). Once the ANN is trained for the first time, evaluation of objective function values is done by using both ANN and the full model (steps 10–13 in Fig. 1). At first, objective values of all chromosomes in the offspring population are evaluated by using the ANN. Then the offspring chromosomes are compared to the ones previously stored in the cache. If the offspring chromosome is found in the cache then its accuracy objective value (approximated by the ANN) is replaced with the corresponding value from the cache (estimated previously by the full model).

To improve the algorithm convergence, a (small) number of chromosomes in the offspring population is selected and re-evaluated by using the full model (if they were previously evaluated by the ANN). The chromosomes selected are the ones present in the best *NF* Pareto (sub)fronts, i.e. subpopulations of the offspring population.

Furthermore, when using the integer coding, two or more genes in a newly created chromosome may have the same value indicating that more than one pressure logger should be placed on the same network node, i.e. indicating an infeasible solution. Even though they should be rejected, such chromosomes are considered by the MOGA–ANN model because of the errors in ANN predictions and, as a consequence, these solutions may still appear in the best *NF* Pareto (sub)fronts. Although applying the above re-evaluation would cause such infeasible solutions to be rejected quickly, it would lead to a weak convergence of the algorithm. To avoid this, a penalty is added to the accuracy objective function value of these chromosomes.

Once the offspring population is created by using the above procedure, it is combined with the parent population into a single population (double the original size). The next generation population (of the original size) is then created by using the standard NSGA-II approach. At this point an additional check is made and if a chromosome fitness value is estimated by the ANN, its fitness is re-evaluated by using the full model. This is necessary to ensure good algorithm convergence and it typically involves a small number of chromosomes. The above search process continues until some convergence criterion is met.

In addition to standard NSGA-II parameters, MOGA–ANN has some additional parameters which have to be set before performing the optimization run. This includes setting the values of *NF*, the number of Initial Training Generations (*ITG*), the number of retraining data and the number of neurons in a hidden layer. The MOGA–ANN is first rigorously analysed in a hypothetical case study to identify the optimal MOGA–ANN model parameter values. These parameter values are then used in a real case study.

4.3.1. Best ranked Pareto (sub)fronts (subpopulations)

As noted above, after identifying all Pareto sub-fronts in the offspring population, members of the best *NF* fronts are checked to see whether their fitness has been calculated by the full model. If not, they are re-calculated using the full model. Obviously, a trade-off exists here – the larger the *NF* is, the better the results will be achieved from the search accuracy point of view, but also more computational time will be required to obtain them.

4.3.2. Number of initial training generations (ITG)

A number of initial full model fitness evaluations are required to obtain data for the first ANN training. This data is collected by using the full fitness model only when evaluating chromosomes in the first *ITG*. A sensitivity analysis is performed to determine the minimum number of *ITG* required for the good MOGA–ANN performance.

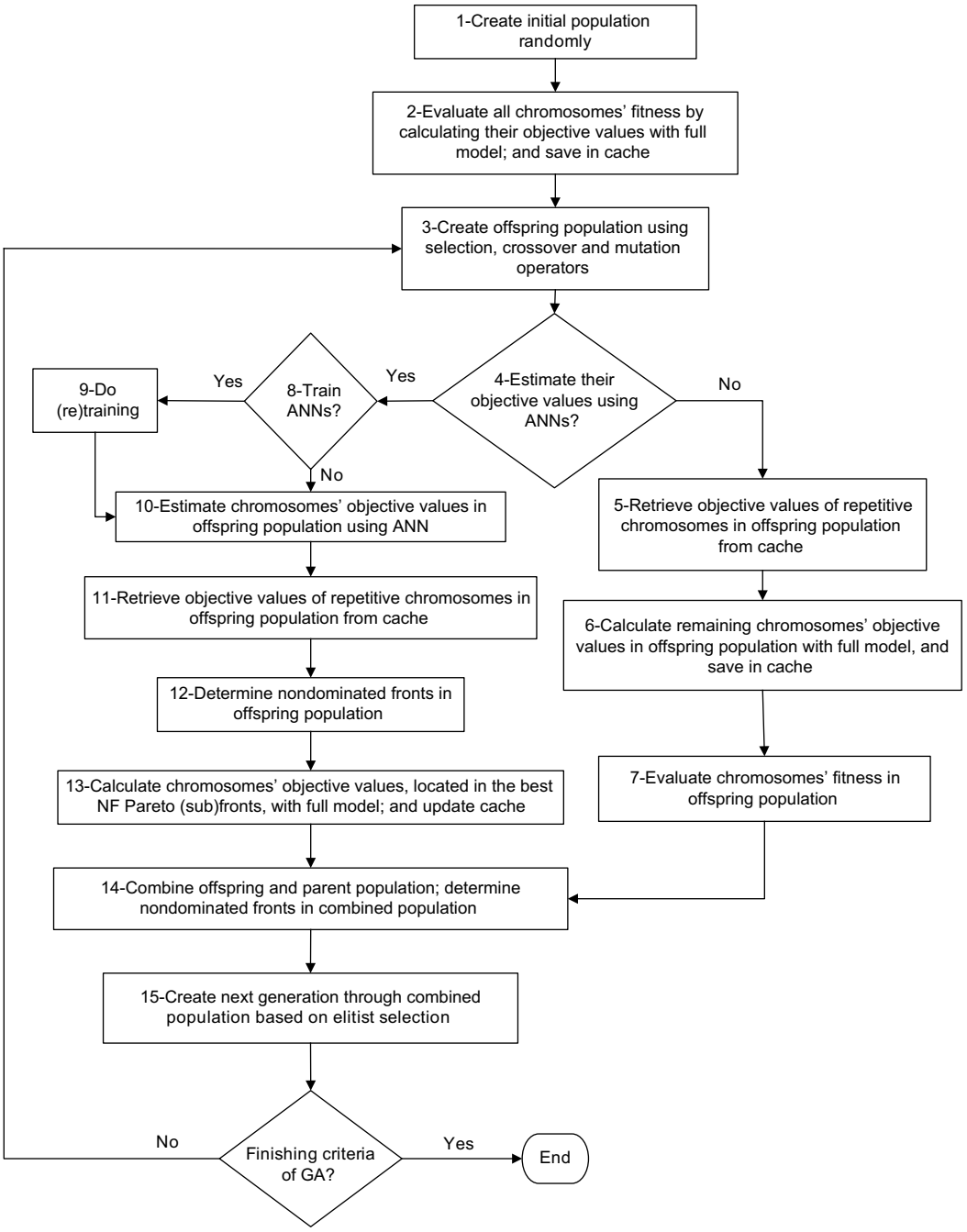

Fig. 1. MOGA–ANN flowchart.

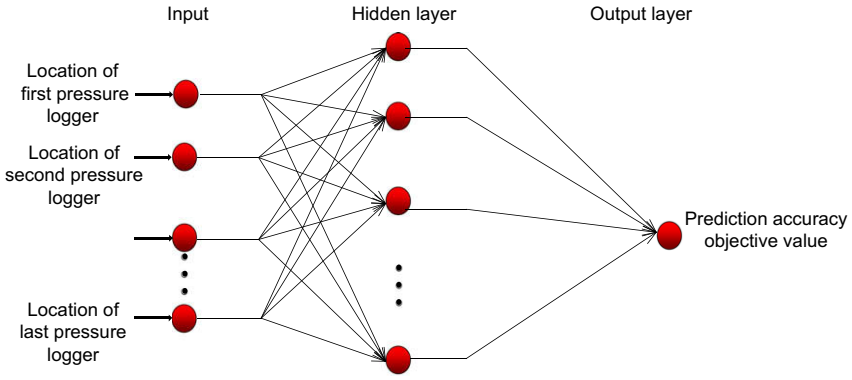

Fig. 2. ANN architecture.

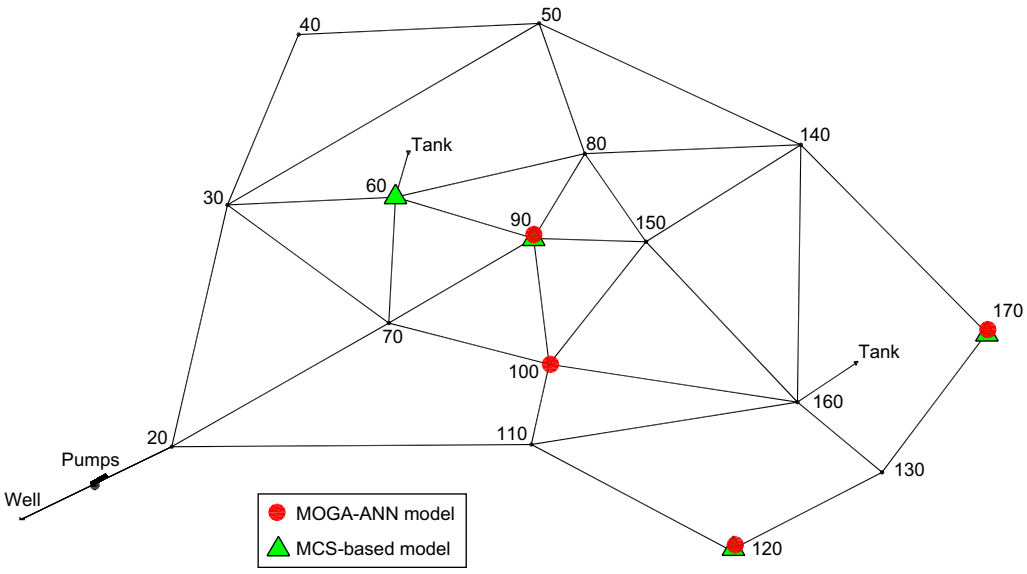

Fig. 3. Case #1: Anytown network layout and optimal pressure logger locations (4 measurement points).

4.3.3. Number of retraining data

To increase the accuracy of ANN predictions, ANNs need to be periodically retrained with new data. The number of retraining data points is defined as the number of additional (i.e. new) full fitness model evaluations that is collected before ANN is (re)trained. There are two possible approaches for collecting additional training data (Yan and Minsker, 2006): (1) the growing set approach and (2) the fixed set approach. In the former approach, the ANN retraining is accomplished with both new and existing data (each time the ANN is retrained) whilst in the latter approach existing data are replaced with new data (leading to the constant number of retraining data and hence, smaller data sets than in the growing set approach). Thus, the fixed set approach typically needs less time for retraining and contains less data but may lead to lower prediction accuracy. A novel mix of the above two approaches is adopted here to exploit the benefits of both. The growing set approach is used first to gather (re)training data until some pre-defined data capacity is reached. After this, new data are replaced with the oldest existing data which are less likely to be found by the genetic algorithm search.

5. Case studies

5.1. Case #1: literature example

The above methodology is first tested and verified on a literature benchmark case study of the Anytown network shown in Fig. 3 (Kapelan et al., 2003). The objective is to compare the computational efficiency and accuracy of the proposed MOGA–ANN method and the MOGA model (the latter being based on full fitness evaluations only, i.e. no use of either ANN or caching).

The network configuration data has been taken from Ormsbee (1989) with the following assumptions. The collected pressure data will be later on used for the calibration of an extended period simulation model with eight steady-state loading conditions. The SD problem is solved with respect to 5 grouped pipe roughness coefficients and 4 grouped nodal demands ($N_a = 9$). All network nodes are considered as potential pressure measurement locations except for the reservoir and tank nodes ($N_{ml} = 16$). Full Jacobian matrix $\mathbf{J}_{ml}$ is obtained by using 16 potential measurement locations and 8 steady-state loading conditions leading to $N_o = 128$. Standard deviation of pressure loggers and number of sample sets are set equal to $s = 0.1$ m and $N_k = 200$ respectively. Uncertain pipe roughness coefficient parameters follow a uniform PDF with lower and upper bounds equal to ±30% of the deterministic value. Uncertain nodal demand parameters follow a Gaussian PDF with coefficient of variation (CV) equal to 0.20.

The following GA parameters are used (values obtained after a limited number of trial runs): population size of 50, binary tournament selection operator, random-by-gene mutation with the probability of 0.25 and single-point crossover with the probability of 0.90. All MOGA and MOGA–ANN runs were performed for 500 generations.

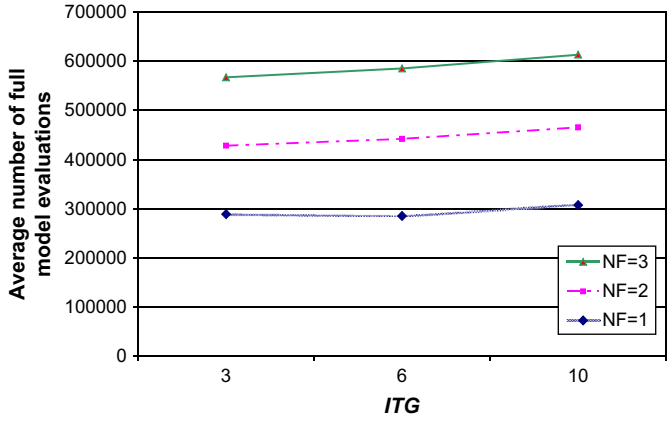

Fig. 4. Case #1: average number of full model fitness evaluations for different values of *NF* and *ITG*.

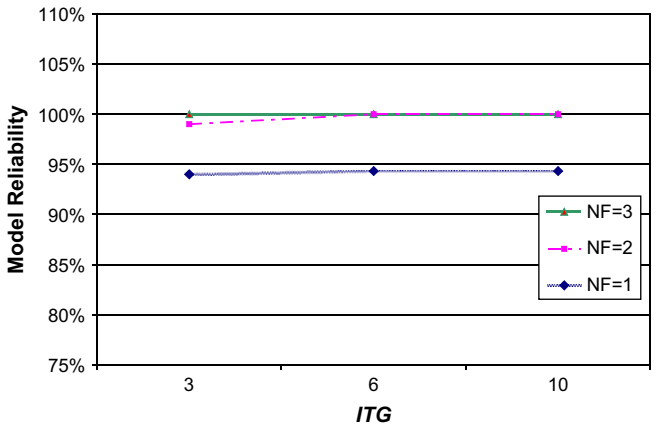

Fig. 5. Case #1: model reliability for different values of *NF* and *ITG*.

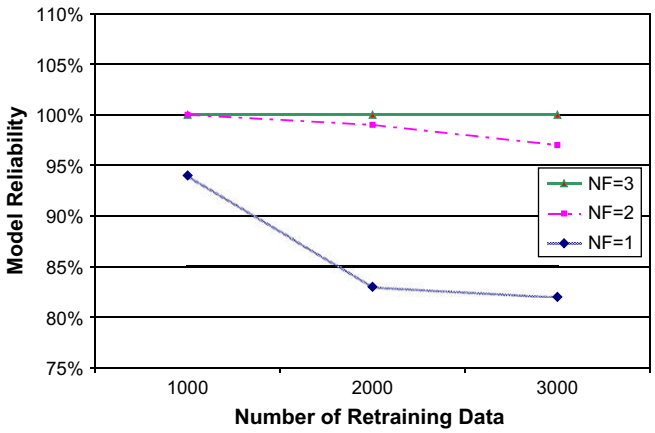

Fig. 6. Case #1: model reliability for different values of *NF* and the number of retraining data.

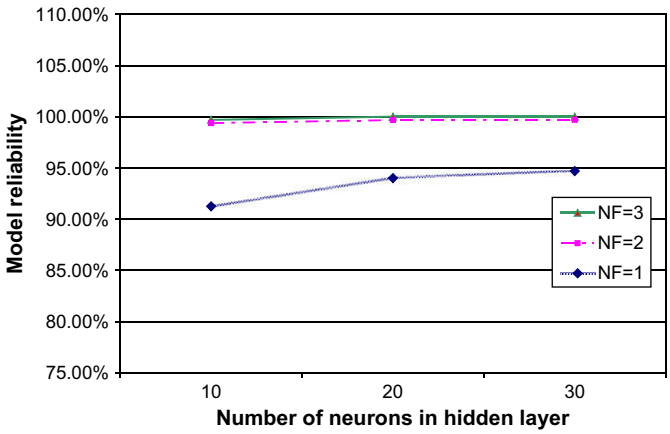

Fig. 7. Case #1: model reliability for different values of *NF* and the number of hidden layer neurons.

MOGA–ANN algorithm parameters were determined by the sensitivity analyses. The criteria for comparing different sets of parameter values are the number of full fitness evaluations and the search model reliability. The latter is denoted here as the percentage of Pareto optimal front points obtained by using the MOGA–ANN model when compared to the MOGA model. This percentage has been averaged over 20 MOGA runs with different random initial populations. The number of best ranked Pareto (sub)fronts (*NF*) is examined especially since it has a major effect on both comparison criteria.

Fig. 4 shows the average number of full model evaluations for three values of *NF* and *ITG*. As it can be seen, when the *NF* is increased, the average number of full model evaluations increases monotonically, and yet, considerably compared to the increasing *ITG*. Fig. 5 shows the model reliability sensitivity with respect to the two MOGA–ANN parameters. Based on this figure, the best MOGA–ANN performance is achieved for $ITG = 6$ and $NF = 2$ or 3.

Fig. 6 shows the sensitivity of model reliability to the number of retraining data. As it can be seen, for $NF = 1$ and 2, model reliability decreases when the number of retraining data increases. This

Table 1
Case #1: Pareto optimal solutions obtained by using the MOGA–ANN and percentage of selected sampling locations obtained by using the MCS-based model.

Number of Monitoring Nodes	F2	F1		Node ID															
				20	30	40	50	60	70	80	90	100	110	120	130	140	150	160	170
2	0.125	0.1618	Opt. locations	0	0	0	0	0	0	0	1	0	0	1	0	0	0	0	0
		0.0484	Percentage	0	1	12	10	20	7	6	14	22	0	72	23	3	1	1	3
3	0.1875	0.2621	Opt. locations	0	0	0	0	0	0	0	1	1	0	1	0	0	0	0	0
		0.2569	Percentage	0	0	13	6	48	6	5	33	55	13	74	33	3	2	2	10
4	0.25	0.3912	Opt. locations	0	0	0	0	0	0	0	1	1	0	1	0	0	0	0	1
		0.3598	Percentage	0	0	2	1	46	18	4	75	42	40	87	21	1	3	14	49
5	0.3125	0.5143	Opt. locations	0	0	0	0	0	0	0	1	1	1	1	0	0	0	0	1
		0.5404	Percentage	0	0	1	1	63	18	0	95	38	74	95	3	0	1	27	86
6	0.375	0.6491	Opt. locations	0	0	0	0	1	0	0	1	1	1	1	0	0	0	0	1
		0.6306	Percentage	0	0	5	0	90	28	1	100	43	90	99	0	0	1	50	96
7	0.4375	0.7198	Opt. locations	0	0	0	0	1	0	0	1	1	1	1	0	0	0	1	1
		0.7198	Percentage	0	0	14	3	99	45	2	100	49	97	100	1	0	1	93	100
8	0.5	0.7731	Opt. locations	0	0	0	0	1	1	0	1	1	1	1	0	0	0	1	1
		0.7731	Percentage	1	0	37	8	100	59	8	100	55	99	100	27	3	5	100	100
9	0.5625	0.8152	Opt. locations	0	0	0	0	1	1	1	1	1	1	1	0	0	0	1	1
		0.8154	Percentage	2	0	51	16	100	71	21	100	68	99	100	53	4	16	100	100
10	0.625	0.8575	Opt. locations	0	0	0	0	1	1	1	1	1	1	1	1	0	0	1	1
		0.8615	Percentage	2	0	63	25	100	83	35	100	84	99	100	76	5	30	100	100
11	0.6875	0.8867	Opt. locations	0	0	0	0	1	1	1	1	1	1	1	1	0	1	1	1
		0.8944	Percentage	4	0	75	35	100	94	49	100	93	100	100	93	8	50	100	100
12	0.75	0.9257	Opt. locations	0	0	1	0	1	1	1	1	1	1	1	1	0	1	1	1
		0.9257	Percentage	5	1	87	57	100	98	64	100	97	100	100	100	12	82	100	100
13	0.8125	0.9561	Opt. locations	0	0	1	1	1	1	1	1	1	1	1	1	0	1	1	1
		0.9561	Percentage	8	2	96	80	100	99	89	100	100	100	100	100	30	99	100	100
14	0.875	0.9771	Opt. locations	0	0	1	1	1	1	1	1	1	1	1	1	1	1	1	1
		0.9771	Percentage	10	8	100	96	100	100	100	100	100	100	100	100	88	100	100	100
15	0.9375	0.9924	Opt. locations	0	1	1	1	1	1	1	1	1	1	1	1	1	1	1	1
		0.9924	Percentage	19	82	100	100	100	100	100	100	100	100	100	100	100	100	100	100

In the "Opt. locations" rows, "1" means pressure logger should be installed in the node and "0" means no pressure logger is required in the node.

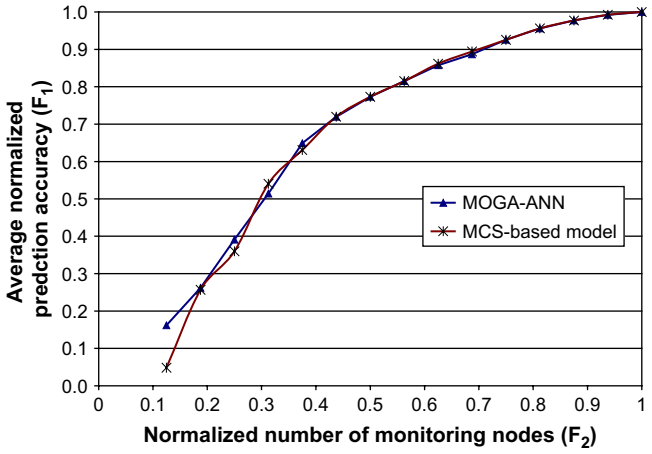

Fig. 8. Case #1: comparison of the Pareto optimal fronts obtained by the MOGA–ANN and the MCS-based models.

decrease for $NF = 1$ is about 10% when the number of retraining data is increased from 1000 to 2000 because ANNs are not updated after their first training. However, the same decrease in model reliability is much lower for $NF = 2$ because ANNs are retrained during the search process and hence the required training data for $NF = 2$ is obtained earlier than the corresponding data for $NF = 1$. For $NF = 3$, model reliability is not dependent on the number of retraining data (always 100%) showing that the value of $NF = 3$ is large enough to cover all errors arising from different ANN updating.

Fig. 7 shows the sensitivity of model reliability to the number of neurons in ANN's hidden layer. As can be seen, model reliability of 100% is obtained for $NF = 2$ and the number of neurons equal to 20 and 30 and $NF = 3$ (regardless of the number of hidden layer neurons). Since a larger number of hidden neurons would lead to longer ANN training times, the number of hidden layer neurons equal to 20 is selected here.

Table 2
Case #1: statistics of normalized pressure prediction accuracy (Equation (5)) for four optimal measurement locations obtained by using the MOGA–ANN and the MCS-based models.

Description	MOGA–ANN	MCS
Mean	0.3912	0.3598
Minimum	0.1146	0.1075
Maximum	0.5414	0.5985
Standard deviation	0.0499	0.0645
95% confidence interval upper bound	0.2804	0.2387
95% confidence interval lower bound	0.4789	0.4857

Based on the above sensitivity analyses, the following MOGA–ANN specific parameter values are used here: $ITG = 6$, $NF = 3$, number of ANN hidden layer neurons = 20 and ANN retraining every 1000 full model fitness evaluations.

To validate and compare the results (i.e. the optimal sampling locations) obtained by using the MOGA–ANN model, the Monte Carlo Simulation (MCS) based model is developed and used here. In the MCS-based model, an equivalent deterministic sampling design optimization problem (i.e. maximization of normalized prediction accuracy defined by equation (5)) is solved for a number of randomly generated calibration parameter samples. Optimal sampling locations are then determined by identifying the most frequently selected sampling locations in these optimization runs. Based on the separate sensitivity analysis performed (not shown here), 200 samples were deemed sufficient for the MCS model.

The optimal sampling locations obtained by the MOGA–ANN model are shown in Table 1. The table also shows the percentage of selected sampling locations obtained by the MCS-based model. As it can be seen, the most frequently selected sampling locations in

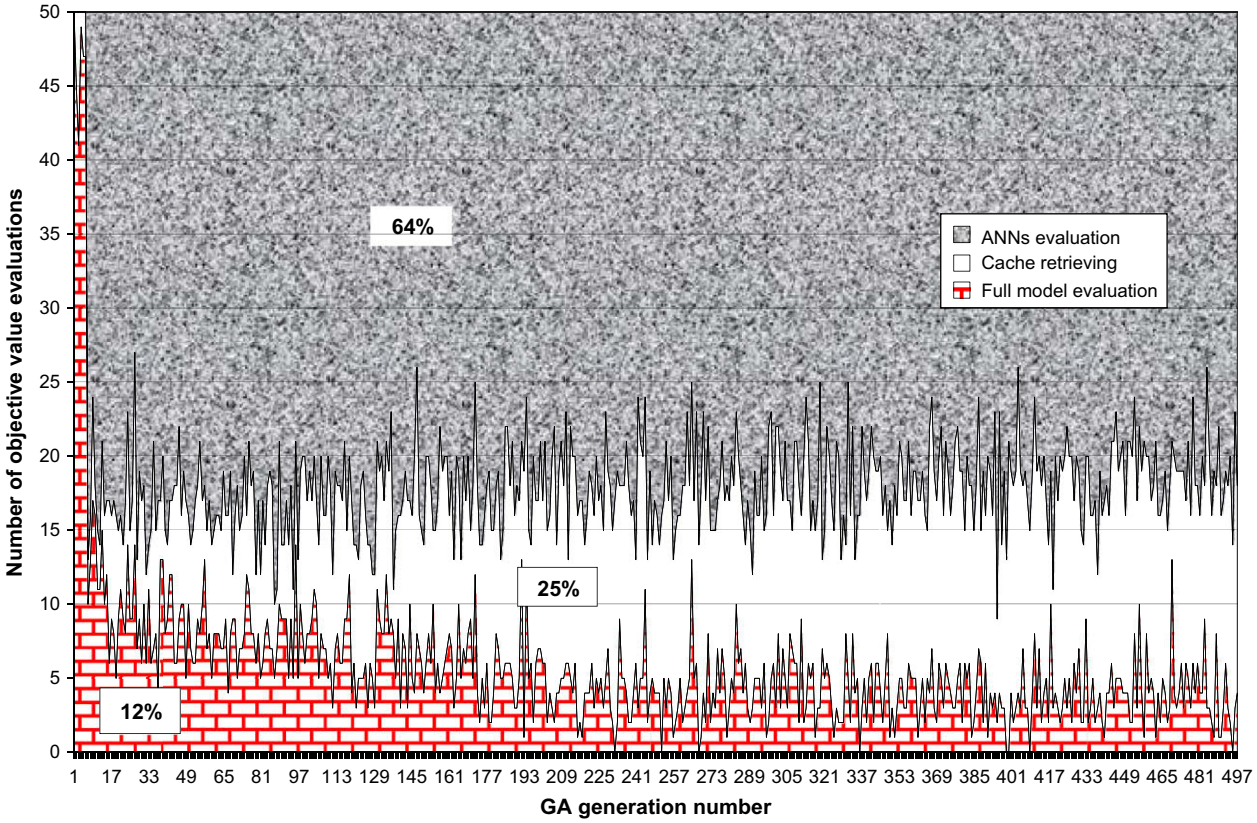

Fig. 9. Case #1: comparison of different type fitness evaluations in MOGA–ANN.

Table 3
Case #1: comparison of computational times.

Model type	Computational time (minutes)	The number of deterministic prediction accuracy calculation calls[a]
MOGA	32	5,000,000
MOGA–ANN	4	590,000
MCS-based	32	5,000,000

[a] The number of deterministic prediction accuracy calculation calls defined by (4) for MOGA and MCS-based model is equal to $N_{pop}N_{gen}N_k$, where N_{pop} is GA population size (50 here) and N_{gen} is the number of GA generation before convergence (500 here) and N_k is the number of samples (200).

the MCS-based model (framed fields) almost always correspond to the optimal ones determined by the MOGA–ANN model. Of course, some discrepancies exist too (dark coloured fields). The differences occur inevitably due to the different approaches used in the two methods when dealing with uncertainty. Nevertheless, 93% of solutions matched show similarity in the results obtained using the above two stochastic approaches. Note that the MOGA model found the same solutions as the MOGA–ANN model and hence its optimal measurement locations are not shown in Table 1.

Furthermore, for each given number of monitoring devices in Table 1, a relatively uniform distribution of optimal measurement locations is seen within the network. This can be interpreted as the tendency of the model to cover all parts of the network. However, these devices are usually located in places far from transmission pipes which are often close to main sources. For example, nodes 20 and 30, which connect the main source and the main costumers, consistently rank low. On the other hand, nodes which are the final receivers of water are the most sensitive nodes and hence they can be the first candidates for selection. For example, the flow in all connecting pipes linked to nodes 90, 120 and 170 is almost always directed towards these nodes, which indicates that they do not transmit water. This can be because such nodes are the most sensitive ones with respect to the head loss changes.

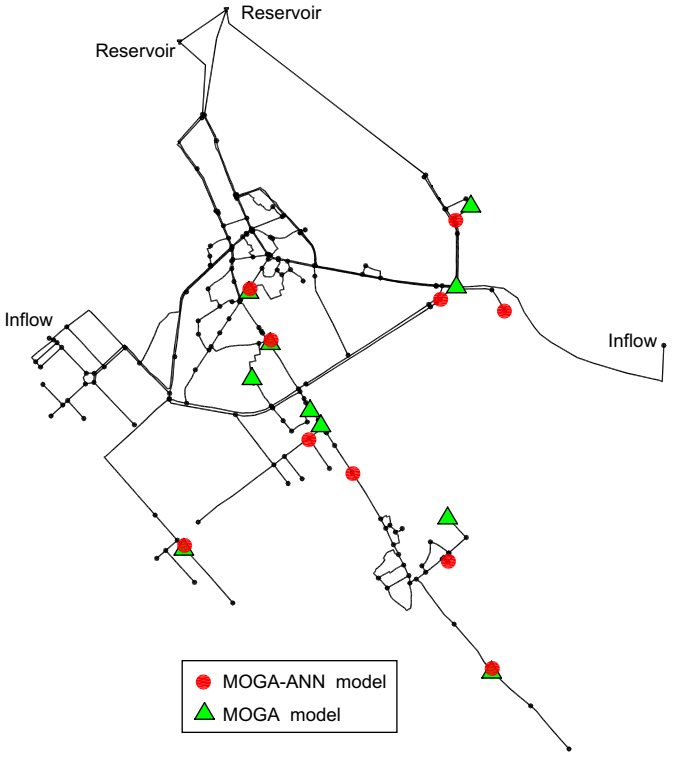

Fig. 10. Case #2: skeletonised Mahalat WDS model and optimal pressure logger locations (10 measurement points).

Table 4
Case #2: summary of pipe materials and diameters.

No.	Original material	Number of pipes	Diameter (mm)
1	Asbestos Cement	406	80–250
2	Ductile iron	470	100–500
3	Galvanized Iron	113	25–125
4	PVC	657	25–110
5	Steel	166	20–65

To compare the Pareto optimal front obtained by the MOGA–ANN and the MCS-based models, solutions are further evaluated in the same uncertain environment. To do so, the following steps are preformed: (1) 10,000 sets of uncertain parameter values are randomly generated according to the pre-specified parameter PDFs; (2) for each model the normalized prediction accuracy (see equation (6)) is calculated for each optimal measurement location identified in the 10,000 samples.

Fig. 8 shows Pareto optimal fronts obtained by the aforementioned method for the two stochastic models. The prediction accuracy of both models is also shown in the third column of Table 1. As can be seen from Fig. 8, both Pareto optimal fronts match reasonably well although MOGA–ANN's front seems to be slightly better for a few measurement locations. Also, note that the largest incremental change in the calibration accuracy is gained when moving from a solution with 6 loggers to a solution with 7 loggers. This fact could be used to select the solution with 7 loggers as the 'best' one, i.e. the most cost-effective one (Kapelan et al., 2005b).

To further compare solutions obtained by the MOGA–ANN and MCS-based models, the four optimal monitoring locations identified by each of these two methods are shown in Fig. 3. Here it shows that three out of four monitoring locations are identical. The statistics of normalized pressure prediction accuracy (see equation (5)) which resulted from model simulations in the uncertain environment are given in Table 2. It can be seen that both statistics are similar to each other.

Fig. 9 shows the comparison of the number of the actual function evaluations using the full model, the caching technique and the ANN approximations as the MOGA–ANN model search progresses. It can be seen from this figure that a total of 12% of chromosomes are evaluated by using the full fitness evaluation model. Most of these evaluations occur in the first six generations of the MOGA–ANN model when the initial ANN training data is obtained. After that, the proportion of the full model evaluations decreases in favour of two other means of estimating the solution fitness. The

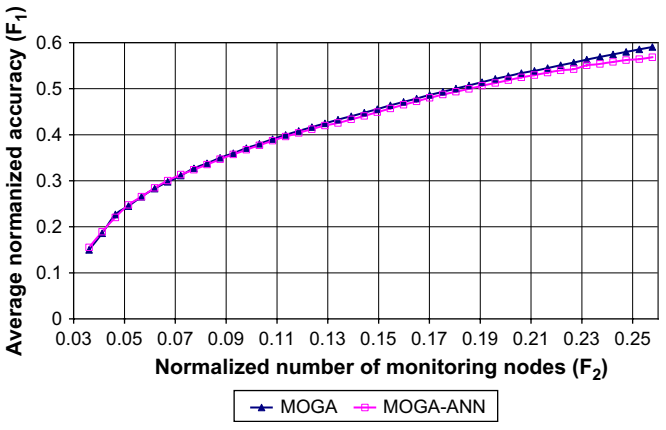

Fig. 11. Case #2: comparison of Pareto optimal fronts obtained by the MOGA and the MOGA–ANN models.

Table 5
Case #2: statistics of normalized pressure prediction accuracy (Equation (5)) and uncertainty (Equation (4)) for ten optimal measurement locations obtained by using MOGA and MOGA–ANN.

Model type	Relative pressure prediction accuracy			Pressure prediction uncertainty (m)		
	Mean	95% confidence interval lower bound	95% confidence interval upper bound	Mean	95% confidence interval lower bound	95% confidence interval upper bound
MOGA	0.2451	0.1836	0.2761	0.6774	0.5838	0.9012
MOGA–ANN	0.2445	0.1849	0.2747	0.6780	0.5909	0.8919

percentage of objective values retrieved from the cache is almost constant at 25% once the initial ANN training is done.

Table 3 shows the comparison of computational effort for the three aforementioned stochastic sampling design models. As can be seen from the second column of this table, the MOGA–ANN model achieves optimal solutions 8 times faster (87% savings) than the MOGA and the MCS-based models.

5.2. Case #2: real-world case study

Here, the proposed MOGA–ANN sampling design model is further tested and verified on the Mahalat WDS shown in Fig. 10. The city of Mahalat is located in the central part of Iran. The WDS covers an area of approximately 46 km^2, with a population of around 160,000. The city is located on a steep slope with the lowest elevation of 1584 m.a.s.l. while the highest elevation is 1900 m.a.s.l. Water demands are predominantly domestic with some commercial users. To reduce the high pressure head induced by the steep slope, six pressure reducing valves (PRVs) are used to decrease pressure heads to pre-specified values. The total number of pipes defined in the original WDS is 1814 with the total length of approximately 101 km.

The dominant pipe materials (see Table 4) are ductile iron (larger pipe diameters), PVC (small diameter pipes) and asbestos cement (most of the middle diameter pipes). The skeletonised EPANET hydraulic model has 237 pipes, 195 junctions, 2 tanks and 6 PRVs. The WDS is supplied by gravity and pumped from three wells and two service tanks (reservoirs). The position of the water supply sources (two wells) is marked in Fig. 10 as 'inflow'. The third well supplies the two reservoirs. The average water demand in the network is 158.9 l/s.

It is assumed that the above WDS model will be calibrated for 7 grouped pipe roughness coefficients, i.e. $N_a = 7$. Although there are a large number of pipes (237 pipes), the small number of calibration parameter groups is assumed to primarily keep the calibrated model prediction error low but also to reduce the computational effort (Mallick et al., 2002). The Hazen Williams (HW) pipe roughness coefficients were first grouped using engineering tables and proposed relationships based on the diameter, material, lining and age of pipes (Walski et al., 1988; Kapelan, 2002). Then, the final pipe grouping was performed by dividing the range of identified HW pipe roughness coefficients (78–155) into the following groups: (78, 90], (90, 100], (100, 110], (110, 120], (120, 130], (130, 140] and (140, 155]. Once this was done, the average value at each interval was considered as the group's representative roughness coefficient value. Furthermore, it was assumed that the Mahalat model would be calibrated for average demand loading conditions only. The standard deviation of all pressure loggers was assumed equal to $s = 1.0$ m.

Since the number of calibration parameters is equal to 7 ($N_a = 7$), the constraint on the minimum number of measurement devices ($N_{\min}$) is set to 7. This ensures that the sampling design solution will lead to at least an even-determined calibration problem. Furthermore, each node of the network was considered as a potential measurement location ($N_{ml} = 195$). However, the maximum number of 50 measurements ($N_{\max} = 50$) was introduced as the SD budget limit. The full Jacobian matrix $\mathbf{J}_{ml}$ is obtained by using all potential measurement locations and average demand loading conditions leading to $N_o = 195$. Note that pressure under average demands can be accurately predicted in this case because the SD problem was solved under average demand conditions.

MOGA model settings were determined after a limited number of trial runs with different initial populations. The following settings have been used for GA parameters in all model runs: population size of 200, binary tournament selection, random-by-gene mutation with probability rate of 0.05 and single-point crossover with probability rate of 0.80. All MOGA runs were performed for 8000 generations. The additional MOGA–ANN model parameters were set equal to the values obtained in the first case study. When compared to this case study, the maximum training data capacity needs to be defined in this case because of the large number of full fitness evaluations. Therefore, the caching capacity of 5000 was assumed for the Mahalat case study. Furthermore, the following assumptions are made about uncertain parameters: (1) the calibration parameters are assumed to be only pipe roughness coefficients, all following a uniform PDF with lower and upper bounds equal to ±30% of the deterministic value; (2) uncertain nodal demands following a Gaussian PDF with coefficient of variation (CV) equal to 0.3 were modelled too (but not calibrated for).

The near optimal measurement locations are obtained by running both the MOGA and the MOGA–ANN models. As the lists of these sampling locations are long (between 7 and 50), only the Pareto optimal fronts obtained are shown here. The same methodology used in case #1 is used here to compare the two Pareto optimal fronts.

Fig. 11 shows the Pareto optimal fronts obtained by the MOGA and the MOGA–ANN models. The following can be observed: (1) both fronts match reasonably well although there is a minor advantage of MOGA over MOGA–ANN for the large number of monitoring locations. As a consequence, solutions obtained by the MOGA–ANN model represent a good surrogate of the solutions obtained by using the MOGA model; (2) an average normalized accuracy of approximately 60% is attainable by monitoring 25% optimal measurement locations (i.e. by using 50 pressure loggers); (3) the rate of increase in WDS model prediction accuracy declines quickly with the increase in number of monitoring locations; for example, adding one more measurement location when 4% locations are already monitored improves the normalized calibrated WDS model prediction accuracy by 3%, while adding one more sampling location when 10% of the system is monitored leads to an improvement (in normalized WDS model prediction accuracy) of less than 1%.

Table 6
Case #2: comparison of the computational times required to obtain Pareto optimal solutions.

Model type	Computational time (minutes)	The number of deterministic prediction accuracy calculation calls[a]
MOGA	1550	320,000,000
MOGA–ANN	65	2,098,400

[a] The number of deterministic prediction accuracy calculation calls defined by (4) for MOGA is equal to $N_{pop}N_{gen}N_k$, where N_{pop} is GA population size (200 here) and N_{gen} is the number of GA generation before convergence (8000 here) and N_k is the number of samples (200).

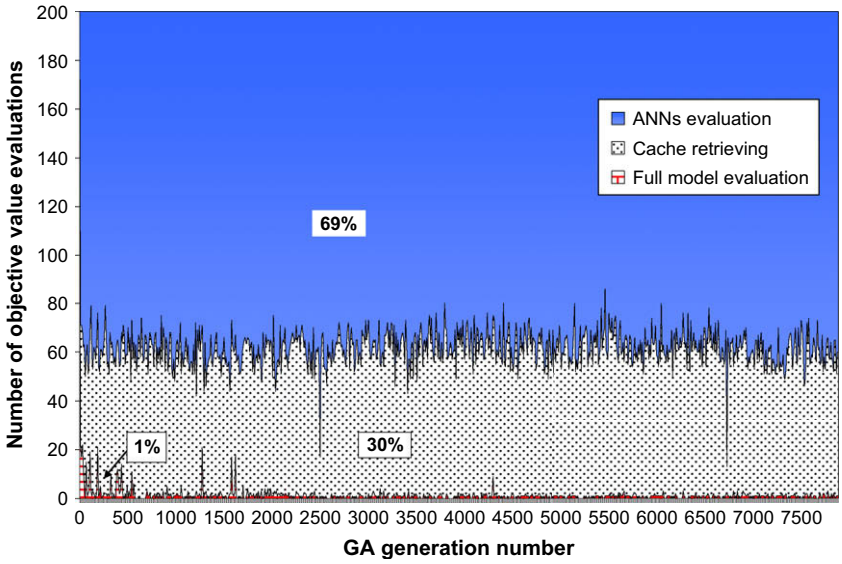

Fig. 12. Case #2: comparison of different fitness type evaluations in the MOGA–ANN model.

The ten MOGA–ANN and MOGA optimal monitoring locations are shown in Fig. 10. Only four monitoring locations are identical although other monitoring nodes are relatively close to each other. The statistics of normalized pressure prediction accuracy (equation (5)) and pressure prediction uncertainty (equation (4)) obtained by using the model simulation in the uncertain environment are given in Table 5. The 95% confidence interval for pressure prediction is between 0.18 and 0.27 in both models. The statistics show similar relevant objective values although the optimal monitoring nodes are not quite the same. This is probably due to the fact that as in many other large-size optimization problems, there are many combinations of near optimal solutions (i.e. monitoring locations) that can produce similar fitness statistics. Fig. 10 also shows that the distribution of ten optimal measurement devices is relatively uniform within the network. The selected measurement locations are usually located away from the main sources and transmission pipes. This confirms that the optimal measurement locations satisfy suggestions put forward by Walski (1983) and verified by Kapelan et al. (2003).

Table 6 shows the comparison of computational times for the two stochastic SD models. It can be seen in the case of a real-world problem, that the main advantage of the MOGA–ANN model when compared to the MOGA model, is that Pareto optimal solutions are obtained with large computational savings (96% approximately) without significant decrease in accuracy.

Finally, Fig. 12 shows the proportion of different types of fitness evaluations performed by the MOGA–ANN model in the case of the Mahalat WDS. This figure shows that less than 1% of all fitness evaluations are performed by using the full model, 65% are performed by using the ANN and the rest is obtained by using the caching technique.

6. Summary and conclusions

This paper addresses the problem of stochastic WDS sampling design for calibration. The objective is to identify best measurement locations in the WDS that should be used to collect the relevant data for subsequent model calibration. The sampling design is formulated and solved as a two-objective optimization problem under calibration parameter uncertainty. The two objectives are the maximization of the calibrated model accuracy and the minimization of the number of sampling devices used (used as a surrogate for sampling design cost). Uncertain calibration parameters are characterised by means of pre-specified PDFs.

The sampling design problem is solved by the new MOGA–ANN algorithm. This is a modified NSGA-II algorithm, which makes use of artificial neural networks and the caching technique to reduce the computational burden. The periodically retrained ANNs are used as surrogate models during the optimization process to speed up the fitness evaluations. The caching technique is used to retrieve previously evaluated solutions efficiently and prevent re-evaluation.

The MOGA–ANN algorithm is tested and verified on two case studies, the benchmark problem of a hypothetical network (Anytown), and the real case study of the Mahalat WDS. The results obtained clearly demonstrate that substantial computational savings can be achieved by using the MOGA–ANN model without significant loss of accuracy. This is a promising result when it comes to solving stochastic sampling design or generally time-consuming multi-objective optimization problems for large-scale WDSs. Having said this, further research work is required to test and verify the capability of the proposed approach before achieving that goal. In addition, improvements achieved by stochastic sampling design should be further investigated in real case studies.

References

Alp, M., Cigizoglu, H.K., 2007. Suspended sediment load simulation by two artificial neural network methods using hydrometeorological data. Environmental Modelling and Software 22 (1), 2–13.

Aly, A.H., Peralta, R.C., 1999. Optimal design of aquifer cleanup systems under uncertainty using a neural network and a genetic algorithm. Water Resources Research 35 (8), 2523–2532.

AWWA, 1999. Calibration guidelines for water distribution system modeling. In: Proceedings of AWWA ImTech Conference.

Berry, J.W., Fleischer, L., Hart, W.E., Phillips, C.A., Watson, J.P., 2005. Sensor placement in municipal water networks. Journal of Water Resources Planning and Management, ASCE 131 (3), 237–243.

Berry, J.W., Hart, W.E., Phillips, C.A., Uber, J.G., Watson, J.P., 2006. Sensor placement in municipal water networks with temporal integer programming models. Journal of Water Resources Planning and Management, ASCE 132 (4), 218–224.

Bhave, P.R., 1988. Calibrating water distribution network models. Journal of Environmental Engineering 114 (1), 120–136.

Blanning, R.W., 1975. The construction and implementation of metamodels. Simulation 24 (6), 177–184.

Broad, D.R., Dandy, G.C., Maier, H.R., 2005. Water distribution system optimization using metamodels. Journal of Water Resources Planning and Management, ASCE 131 (3), 172–180.

Bush, C.A., Uber, J.G., 1998. Sampling design methods for water distribution model calibration. Journal of Water Resources Planning and Management, ASCE 124 (6), 334–344.

Deb, K., Pratap, A., Agarwal, S., Meyarivan, T., 2002. A fast and elitist multiobjective genetic algorithm: NSGA-II. IEEE Transactions on Evolutionary Computation 6 (4), 182–197.

de Schaetzen, W., Walters, G.A., Savic, D.A., 2000. Optimal sampling design for model calibration using shortest path, genetic and entropy algorithms. Urban Water 2, 141–152.

Farmani, R., Savic, D.A., Walters, G.A., 2003. Benchmark problems for design and optimisation of water distribution systems. In: Maksimovic, C., Butler, D., Memon, F. (Eds.), Advances in Water Supply Management. A.A. Balkema Publishers, pp. 249–256.

Ferreri, G.B., Napoli, E., Tumbiolo, A., 1994. Calibration of roughness in water distribution networks. Proceeding of second International Conference on Water Pipeline Systems, 1, D. S. Miller, (Ed.), PEP, Suffolk, U.K., 379-396.

Helton, J.C., Davis, F.J., 2003. Latin hypercube sampling and the propagation of uncertainty in analyses of complex systems. Reliability Engineering and System Safety 81, 23–69.

Kapelan, Z., 2002. Calibration of WDS Hydraulic Models. PhD thesis, School of Engineering and Computer Science, Univ. of Exeter, Exeter, U.K.

Kapelan, Z., Savic, D.A., Walters, G.A., 2003. Multi-objective sampling design for water distribution model calibration. Journal of Water Resources Planning and Management 129 (6), 466–479.

Kapelan, Z., Savic, D.A., Walters, G.A., 2005a. Optimal sampling design methodologies for water distribution model calibration. Journal of Hydraulic Engineering 131 (3), 190–200.

Kapelan, Z., Savic, D.A., Walters, G.A., 2005b. Multiobjective design of water distribution systems under uncertainty. Water Resources Research 41 (11), W11407, doi:10.1029/2004WR003787.

Lansey, K.E., 2006. The evolution of optimizing water distribution system applications. In: 8th Annual Water Distribution Systems Analysis Symposium, Cincinnati, Ohio, USA.

Lansey, K.E., Basnet, C., 1991. Parameter estimation for water distribution networks. Journal of Water Resources Planning and Management, ASCE 117 (1), 126–144.

Lansey, K.E., EL-Shorbagy, W., Ahmed, I., Araujo, J., Haan, C.T., 2001. Calibration assessment and data collection for water distribution networks. Journal of Hydraulic Engineering 127 (4), 270–279.

Lee, B.H., Deininger, R.A., 1992. Optimal locations of monitoring stations in water distribution system. Journal of Environmental Engineering, ASCE 118 (1), 4–16.

Leshno, M., Lin, V.Y., Pinkus, A., Schocken, S., 1993. Multilayer feed forward networks with a nonpolynomial activation function can approximate any function. Neural Networks 6, 861–867.

Lin, B., Syed, M., Falconer, R.A., 2008. Predicting faecal indicator levels in estuarine receiving waters – an integrated hydrodynamic and ANN modelling approach. Environmental Modelling and Software 23 (6), 729–740.

Lingireddy, S., Ormsbee, L.E., 1998. Neural networks in optimal calibration of water distribution systems. In: Flood, I., Kartam, N. (Eds.), Artificial Neural Networks for Civil Engineers: Advanced Features and Applications. ASCE, Reston, VA, pp. 53–76.

Mallick, K.N., Ahmed, I., Tickle, K.S., Lansey, K.E., 2002. Determining pipe groupings for water distribution networks. Journal of Water Resources Planning and Management, ASCE 128 (2), 130–139.

May, R.J., Dandy, G.C., Maier, H.R., Nixon, J.B., 2008. Application of partial mutual information variable selection to ANN forecasting of water quality in water distribution systems. Environmental Modelling and Software 23 (10–11), 1289–1299.

McKay, M.D., Conover, W.J., Beckman, R.J., 1979. A comparison of three methods for selecting values of input variables in the analysis of output from a computer code. Technometrics 211, 239–245.

Meier, R.W., Barkdoll, B.D., 2000. Sampling design for network model calibration using genetic algorithms. Journal of Water Resources Planning and Management, ASCE 126 (4), 245–250.

Ormsbee, L.E., 1989. Implicit network calibration. Journal of Water Resources Planning and Management, ASCE 115 (2), 243–257.

Ostfeld, A., Salomons, E., 2004. Optimal layout of early warning detection stations for water distribution systems security. Journal of Water Resources Planning and Management, ASCE 130 (5), 377–385.

Piller, O., Bremond, B., Morel, P., 1999. A spatial sampling procedure for physical diagnosis in a drinking water supply network. In: Savic, D.A., Walters, G.A. (Eds.), Proc., Water Industry Systems: Modelling and Optimisation Applications, vol. 1. Univ. of Exeter, Exeter, U.K, pp. 309–316.

Post, J., Hattermann, F.F., Krysanova, V., Suckow, F., 2008. Parameter and input data uncertainty estimation for the assessment of long-term soil organic carbon dynamics. Environmental Modelling and Software 23 (2), 125–138.

Propato, M., 2006. Contamination warning in water networks: general mixed-integer linear models for sensor location design. Journal of Water Resources Planning and Management, ASCE 132 (4), 225–233.

Shastri1, Y., Diwekar, U., 2006. Sensor placement in water networks: a stochastic programming approach. Journal of Water Resources Planning and Management, ASCE 132 (3), 192–203.

Vitkovsky, J.P., Liggett, J.A., Simpson, A.R., Lambert, M.F., 2003. Optimal measurement site locations for inverse transient analysis in pipe networks. Journal of Water Resources Planning and Management, ASCE 129 (6), 480–492.

Walski, T.M., 1983. Technique for calibrating network models. Journal of Water Resources Planning and Management, ASCE 109 (4), 360–372.

Walski, T.M., 1986. Case study: pipe network model calibration issues. Journal of Water Resources Planning and Management, ASCE 112 (2), 238–249.

Walski, T.M., Sharp, W.W., Shields, F.D., 1988. Predicting Internal Roughness in Water Mains. Miscellaneous Paper EL-88–2, US Army Engineer Waterways Experiment Station, Vicksburg, Miss.

Yan, S., Minsker, B., 2006. Optimal groundwater remediation design using an adaptive neural network genetic algorithm. Water Resources Research 42, W05407, doi:10.1029/2005WR004303.

Yu, G., Powell, R.S., 1994. Optimal design of meter placement in water distribution systems. International Journal of Systems Sciences 25 (12), 2155–2166.